Inorganic Chemistry

Article

pubs.acs.org/IC

Hybrid Uranium–Transition-Metal Oxide Cage Clusters

Jie Ling,[†] Franklin Hobbs,[†] Steven Prendergast,[†] Pius O. Adelani,[†] Jean-Marie Babo,[†] Jie Qiu,[†] Zhehui Weng,[†] and Peter C. Burns*[,†,‡]

[†]Department of Civil and Environmental Engineering and Earth Sciences, and [‡]Department of Chemistry and Biochemistry, University of Notre Dame, Notre Dame, Indiana 46556, United States

Supporting Information

ABSTRACT: Transition-metal based polyoxometalate clusters have been known for decades, whereas those built from uranyl peroxide polyhedra have more recently emerged as a family of complex clusters. Here we report the synthesis and structures of six nanoscale uranyl peroxide cage clusters that contain either tungstate or molybdate polyhedra as part of the cage, as well as phosphate tetrahedra. These transition-metal–uranium hybrid clusters exhibit unique polyhedral connectivities and topologies that include 6-, 7-, 8-, 10-, and 12-membered rings of uranyl polyhedra and uranyl ions coordinated by bidentate peroxide in both trans and cis configurations. The transition-metal polyhedra appear to stabilize unusual units built of uranyl polyhedra, rather than templating their formation.

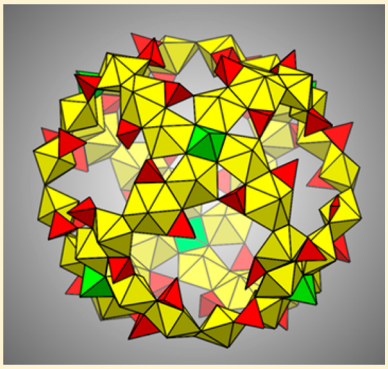

1. INTRODUCTION

Metal-oxide clusters include the vast family of transition-metal based polyoxometalates[1−6] and the more recently discovered uranium-oxide cage clusters based on uranyl peroxide polyhedra.[7−10] We have suggested that the latter may be important products of the interaction of damaged nuclear fuel with water (including seawater such as at Fukushima, Japan) because the interaction of radioactivity with water creates the peroxide that is necessary for formation of these clusters.[11,12] Uranyl peroxide clusters may provide important transport mechanisms in geologic disposal scenarios for nuclear waste and possibly even in natural systems. Toward an understanding of the nanoscale behavior of uranium, we have developed and characterized a family of uranyl peroxide cage clusters over the past several years.[8,10]

In addition to the potential importance of uranyl peroxide cage clusters in uranium environmental transport, they also present the possibility of establishing nanoscale control of uranium.[13] An advantage of this may be reduced costs and environmental impact of fabrication of new nuclear fuel and waste forms, as well as for the reprocessing of used nuclear fuel. Recently we have shown that it is possible to apply membrane-based ultrafiltration methods to the recovery of nanoscale uranyl peroxide clusters from aqueous solutions.[14]

We are interested in extending the family of uranyl peroxide cage clusters to include transition metals, thereby creating a new class of nanoscale metal-oxo clusters that are hybrids of the uranyl peroxide and transition-metal polyoxometalate families. In the latter case, tremendous structural diversity has been delineated over the past few decades, and a variety of applications that span materials science, catalysis, and medicine are emerging.[2−4,6,15] A few studies have shown that actinides may be linked to transition-metal clusters,[16−22] several studies examined clusters containing actinides as essential components, together with transition metals,[23−26] and we recently reported a mixed uranyl-tungstate ring-shaped cluster.[27]

Here we provide a report of the synthesis of a novel family of hybrid uranyl transition-metal cage clusters that we have recently isolated and characterized in our laboratory. We focus here on the unique structures and compositions of six hybrid clusters revealed by crystallographic analyses, with particular attention paid to their metal coordination environments and overall connectivities. These clusters are novel because they incorporate transition-metal polyhedra into the walls of cages along with uranyl polyhedra. Previously, uranyl peroxide cages that encapsulate transition-metal polyhedra have been described,[28] as have wheel-shaped clusters consisting of uranyl peroxide polyhedra and tungstate polyhedra.[27]

2. EXPERIMENTAL SECTION

2.1. Cluster Synthesis. *Caution: Although the* $UO_2(NO_3)_2{\cdot}6H_2O$ *used in these experiments contains isotopically depleted U, precautions for handling radioactive materials should be followed and such work should only be conducted by qualified personnel in suitable facilities.* $UO_2(NO_3)_2{\cdot}6H_2O$ (MV Laboratories, Lot no. P705UA1), aqueous $H_3PW_{12}O_{40}$ (10%, Sigma-Aldrich), aqueous $H_3PMo_{12}O_{40}$ (10%, Sigma-Aldrich), H_2O_2 (30%, Alfa-Aesar), $LiOH{\cdot}H_2O$ (98%, Fisher), and H_3PO_3 (98%, Acros) were used as received. Distilled and Millipore filtered water with a resistance of 18.2 MΩ cm was used in all reactions. We explored aqueous systems containing various uranyl to transition-metal ratios, and pH values. Most did not yield crystals or gave crystals of previously known clusters.

Received: August 1, 2014
Published: December 1, 2014

Table 1. Selected Crystallographic Parameters for the Cage Clusters under Study

	$U_{18}W_2P_{12}$	$U_{28}W_4P_{12}$	$U_{28}Mo_4P_{12}$	$U_{50}W_6P_{20}$	$U_{44}Mo_2P_{16}$	$U_{48}W_6P_{48}$
a (Å)	26.272(3)	20.783(5)	20.7645(14)	22.660(4)	29.395(2)	29.632(3)
b (Å)		20.808(5)	20.7997(14)	26.287(5)	25.553(2)	
c (Å)	21.354(2)	34.724(9)	34.591(2)	39.993(7)	27.939(2)	34.132(4)
α (deg)		76.107(3)	76.443(1)	72.184(3)		
β (deg)		80.701(3)	80.917(1)	88.286(3)		
γ (deg)		80.572(3)	80.419	68.547(2)		
volume (Å^3)	12764(2)	14263(6)	14210(2)	21018(6)	20986(3)	29970(6)
space group	$P6_3/mmc$	$P\bar{1}$	$P\bar{1}$	$P\bar{1}$	$Pmn2_1$	$P4/n$
Z	2	2	2	2	2	2
ind reflections	3045	51495	46920	17404	20663	18816
unique $F_0 > 4\sigma_F$	2636	24169	33545	9905	18115	14893
R_1[a]	0.060	0.112	0.061	0.086	0.057	0.094
wR_2[a]	0.166	0.313	0.185	0.259	0.174	0.242
S	1.09	0.99	1.00	1.00	1.32	1.00

[a] $R_1 = \sum||F_o| - |F_c||/\sum|F_o|$. $Rw_2(F_o^2) = [\sum[w(F_o^2 - F_c^2)^2]/\sum wF_o^4]^{1/2}$.

The uranium transition-metal clusters presented herein are designated as $U_iW_jP_k$ or $U_iMo_jP_k$, where integers i, j, and k designate the number of U, W or Mo, and P atoms present in the cluster, respectively. In all cases the yields of crystals containing the clusters were low, typically only a few crystals.

$U_{50}W_6P_{20}$. $[(UO_2)_{50}(O_2)_{42}(WO_3OH)_6(H_2PO_4)_{20}(OH)_8(H_2O)_{18}]^{18-}$ was synthesized by loading $UO_2(NO_3)\cdot 6H_2O$ (0.5 M, 0.1 mL), H_2O_2 (30%, 0.1 mL), LiOH (2.38 M, 0.1 mL), aqueous $H_3PW_{12}O_{40}$ (10%, 0.1 mL), and H_3PO_3 (0.5 M, 0.12 mL) into a 2 mL glass vial, giving an initial pH of 5.8. The solution was left standing open to air, and $U_{50}W_6P_{20}$ clusters crystallized within 3 weeks. Energy dispersive spectroscopy (EDS, see below) provided an estimated U:W:P atomic ratio of 50:6:22.

$U_{44}Mo_2P_{16}$. $[(UO_2)_{44}(O_2)_{38}(H_2PO_4)_{14}(HPO_4)_2(MoO_3OH)_2(OH)_{15}(H_2O)_{14}]^{23-}$ was synthesized as for $U_{50}W_6P_{20}$, except that an aqueous $H_3PMo_{12}O_{40}$ solution (10%, 0.1 mL) was used instead of $H_3PW_{12}O_{40}$ and 0.1 mL of H_3PO_3 solution was used. The initial solution pH was 6.0, and $U_{44}Mo_2P_{16}$ clusters crystallized within 2 weeks. EDS analysis provided an estimated U:Mo:P atomic ratio of 44:3:20.

$U_{28}W_4P_{12}$. $[(UO_2)_{28}(O_2)_{24}(WO_3OH)_4(H_2PO_4)_{12}(H_2O)_{12}]^{20-}$ was synthesized as for $U_{50}W_6P_{20}$, except that the volume of $H_3PW_{12}O_{40}$ aqueous solution was reduced to 0.05 mL. The initial measured pH was 6.2. $U_{28}W_4P_{12}$ clusters crystallized within 2 weeks. EDS analysis provided an estimated U:W:P atomic ratio of 28:5:14.

$U_{28}Mo_4P_{12}$. $[(UO_2)_{28}(O_2)_{24}(MoO_3OH)_4(H_2PO_4)_{12}(H_2O)_{12}]^{20-}$ was synthesized as for $U_{28}W_4P_{12}$, except that an aqueous $H_3PMo_{12}O_{40}$ solution was used instead of $H_3PW_{12}O_{40}$. The initial measured pH was 6.2. EDS analysis gave an estimated U:Mo:P atomic ratio of 28:5:15.

$U_{18}W_2P_{12}$. $[(UO_2)_{18}(O_2)_{15}(W_2O_6(OH)_3)(H_2PO_4)_{12}(H_2O)_6]^{9-}$ was synthesized as for $U_{50}W_6P_{20}$, except that the volumes of $H_3PW_{12}O_{40}$ and H_3PO_3 solutions were reduced to 0.05 and 0.075 mL, respectively. This resulted in an initial solution pH of 6.5. $U_{18}W_2P_{12}$ clusters crystallized within 2 weeks. EDS analysis gave an estimated U:W:P atomic ratio of 18:2:14.

$U_{48}W_6P_{48}$. $[(UO_2)_{48}(O_2)_{12}(WO_4OH)_6(H_2PO_4)_{24}(HPO_4)_{24}]^{18-}$ was synthesized as for $U_{18}W_2P_{12}$, except that 0.025 mL of $H_3PW_{12}O_{40}$ solution was used. The initial pH of the solution was 8.4 and $U_{48}W_6P_{48}$ clusters crystallized within 2 weeks. EDS analysis gave an estimated U:W:P atomic ratio of 48:8:53.

2.2. Crystal Structure Analysis. Our past experience studying uranyl peroxide cage clusters has demonstrated that crystal-structure determination for such crystals is difficult, and results will be inferior to those generally expected for inorganic solids.[10] Although the positions of the U atoms and their coordinating O atoms are normally well-defined, H_2O groups and counterions located between and inside the clusters are seldom fully determined. Uranium dominates the X-ray scattering, which makes precise determination of O atom locations difficult. Relatively large portions of the crystals contain relatively low electron density, as compared to uranium, and as a result diffraction data are seldom attainable above about 45 deg in two theta (MoKα radiation), and substantial portions of the measured reflections are weak. The locations of H atoms are not attainable, and usually the data do not support refinement of anisotropic displacement parameters for the O atoms or lighter cations. Despite these various shortcomings, X-ray diffraction provides the details of the connectivity of the cage clusters, with U−O bond length errors of about 0.02−0.04 Å, and lacking crystals with dimensions of several millimeters that would be suitable for neutron diffraction, provides the best opportunity to characterize the structures of such clusters.

A sphere of three-dimensional X-ray diffraction data was collected for a suitable crystal corresponding to each cluster at 100 K using a Bruker Platform goniometer, an APEX CCD detector, and MoKα radiation from a conventional sealed-source tube. A semiempirical correction for absorption was applied to the full sphere of data in each case using the program SADABS.[29] Data were integrated using the Bruker APEX II software,[30] and the SHELXTL system of programs[31] was used for solution and refinement of the structures. Selected crystallographic parameters are provided in Table 1; full details are in the Supporting Information. Solvent accessible void space contained within cages $U_{50}W_6P_{20}$, $U_{44}Mo_2P_{16}$, and $U_{28}Mo_4P_{12}$ are 1497, 1247, and 448 Å^3, according to calculations done using the algorithm in Squeeze.

The structure determinations did not provide reliable positions for the Li cations or lattice water, due to the dominance of U in scattering X-rays, and possibly due to disorder. Nyman recently reported that Li cations in specific structures based on clusters of uranyl polyhedra are mobile in the solid state,[32] which could be the case in the currently studied compounds.

Bond-valence sums were calculated[33,34] for each site in each structure. The sums incident at the metal sites are consistent with assigned formal oxidation states, as expected for the oxidizing conditions of the synthesis experiments. The sums incident upon O atoms bonded to uranyl cations were used to assign the corresponding O atom as O^{2-}, OH^-, or H_2O.

2.3. Infrared Spectroscopy. An infrared spectrum was obtained for single crystals containing one of $U_{28}W_4P_{12}$, $U_{48}W_6P_{48}$, $U_{18}W_2P_{12}$, $U_{50}W_6P_{20}$, or $U_{44}Mo_2P_{16}$ using a SensIR technology IlluminatIR FT-IR microspectrometer. A single crystal was placed on a glass slide, and the spectrum was collected with a diamond ATR objective from 650 to 4000 cm^{-1} with a beam aperture of 100 μm. The spectra are given in the Supporting Information. Bands at ~912 cm^{-1} are due to uranyl ion asymmetric stretches, those at ~980 cm^{-1} are due to vibrations of W−O bonds in tungstate, bands in the range of 1000 to 1400 cm^{-1} are attributed to the asymmetric stretching vibrations of P−O bonds, and those in the range of 3000 to 3500 cm^{-1} and a strong band at 1650

dx.doi.org/10.1021/ic5018449 | Inorg. Chem. 2014, 53, 12877−12884

cm^{-1} are assigned to the O−H vibrations in hydroxyl groups (excluding 1650 cm^{-1}) and water molecules.

2.4. Energy Dispersive Spectroscopy. Energy dispersive spectra were collected for single crystals containing each cluster using a LEO EVO-50XVP variable-pressure/high-humidity scanning electron microscopy. Spectra for each compound confirm the presence of U, W/Mo, P, O and gave ratios in approximate agreement with those from the crystal structure determinations. Li cannot be detected using this method.

3. RESULTS

The crystallographic studies indicate that six nanoscale cage clusters consisting of uranyl polyhedra, phosphate tetrahedra, and tungstate or molybdate polyhedra self-assembled in aqueous solution under ambient conditions and subsequently crystallized. In each case cage clusters formed in which the inner and outer walls of the clusters are bounded by the relatively unreactive O atoms of the uranyl ions. The cage clusters are anionic, and it is likely that many of the nonbridging O atoms of the phosphate or transition-metal polyhedra are protonated. Full protonation is assumed for the purposes of stating their chemical formulas here. Any remaining negative charge is balanced in the crystals by Li counter cations that are likely both encapsulated in the cages, and located outside of the clusters. In the subsequent sections we examine the coordination environments of the various cations, and their connectivity into cage clusters.

3.1. Uranyl Coordination Environments. The uranium is hexavalent in each of the clusters reported here, as expected given the experimental conditions, and as shown by the presence of uranyl ions in the crystal structures and prominent modes corresponding to uranyl ion vibrations in the infrared spectra. In all cases the U^{6+} cations are present as typical dioxo $(UO_2)^{2+}$ uranyl cations with U−O bond lengths of ∼1.8 Å and O−U−O bond angles of ∼180°. Each of these uranyl ions is coordinated by five or six ligands that are arranged at the equatorial positions of pentagonal or hexagonal bipyramids, respectively. However, the details of the coordinating ligands is richly diverse in these clusters, with 10 different configurations represented over the various clusters (Figure 1). In three of these, there are two peroxo ligands that are bidentate to the uranyl ion in a cis arrangement, where they form two of the equatorial edges of hexagonal bipyramids (Figure 1a−c). The coordination environments about the uranyl ions in these cases are completed by two hydroxyl ligands (Figure 1a), one hydroxyl ligand and a monodentate $(HPO_4)^{2-}$ ligand (Figure 1b), or two monodentate $(H_2PO_4)^{1-}$ ligands (Figure 1c). Two configurations have uranyl ions with two bidentate peroxo ligands in a *trans* arrangement along equatorial edges of hexagonal bipyramids (Figure 1d,e). In one case, the uranyl ion is also coordinated by a hydroxyl ligand and a H_2O group, with these also in a trans arrangement (Figure 1d). In the other, the coordination environment is completed by one H_2O group as well as either one $(WO_3OH)^{1-}$, one $(MoO_3OH)^{1-}$, or one $(HPO_4)^{2-}$ ligand (Figure 1e). Two uranyl configurations contain a single bidentate peroxo ligand along one equatorial edge of a hexagonal bipyramid (Figure 1f,g). The uranyl polyhedra are completed by two bidentate $(H_2PO_4)^{1-}$ ligands (Figure 1f), or by two hydroxyl ligands in a trans arrangement, as well as one bidentate $(HPO_4)^{2-}$ ligand (Figure 1g). Three configurations contain no peroxo ligands (Figure 1h−j). In these cages, hexagonal bipyramidal coordination environments are created about the uranyl ion by two bidentate $(H_2PO_4)^{-}$ ligands in a cis arrangement as well as two hydroxyl ligands

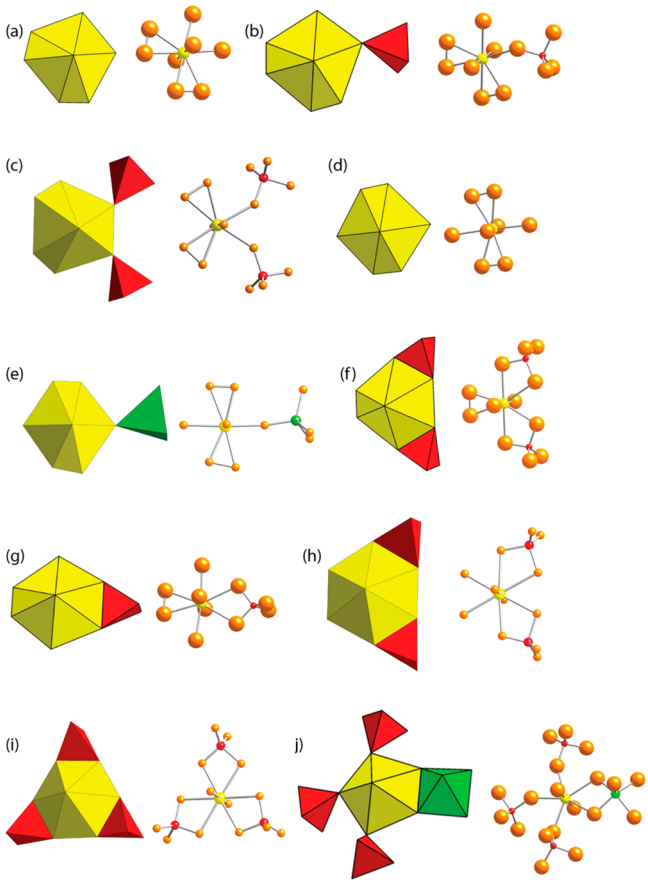

Figure 1. Coordination environments about the uranyl ions in the hybrid uranyl-transition-metal clusters under study. Uranyl bipyramids, phosphate tetrahedra, and tungstate square pyramids are shown in yellow, red, and green, respectively. In the ball-and-stick representations, uranium, phosphorus, transition-metal, and oxygen atoms are shown in yellow, red, green, and orange, respectively.

(Figure 1h), or by three bidentate $(H_2PO_4)^{1-}$ ligands (Figure 1i). A uranyl pentagonal bipyramid includes three monodentate $(HPO_4)^{2-}$ ligands, and a $(WO_4OH)^{3-}$ square pyramid contributes two vertices (Figure 1j). In comparison with other cage clusters built from uranyl peroxide polyhedra, all of these configurations except that shown in Figure 1a are novel.[8]

3.2. Transition Metal Coordination Environments. In $U_{50}W_6P_{20}$, $U_{44}Mo_2P_{16}$, $U_{28}W_4P_{12}$, and $U_{28}Mo_4P_{12}$ all of the transition metals are tetrahedrally coordinated by O/OH. The single symmetrically distinct W^{6+} site in $U_{18}W_2P_{12}$ is in a strongly distorted octahedral coordination environment. Three W−O bond lengths are short at 1.78 Å, and three W−OH bond lengths are 2.18 Å. The calculated bond-valence sum is 5.85 valence units, consistent with the expected formal valence. These W−OH/O bond lengths are comparable to those reported in a variety of uranyl tungstates.[35,36] In $U_{48}W_6P_{48}$, the three symmetrically distinct W^{6+} cations each occur in square pyramidal coordination environments with apical nonbridging hydroxyl.

3.3. Phosphate Coordination Environments. All P cations in the clusters reported herein are coordinated by four O/OH anions in tetrahedral arrangements with typical bond lengths.

3.4. The $U_{50}W_6P_{20}$ Cage Cluster. $U_{50}W_6P_{20}$ is a highly complex cage cluster that consists of 50 uranyl ions, 6 $(WO_3OH)^{1-}$ tetrahedra, and 20 $(H_2PO_4)^{1-}$ tetrahedra (Figure

dx.doi.org/10.1021/ic5018449 | Inorg. Chem. 2014, 53, 12877−12884

2), where protonation of terminal O atoms bonded to W and P is assumed. It also contains 42 peroxo ligands, eight hydroxyl ligands bonded to uranyl ions, and 18 H_2O groups, all that coordinate uranyl ions. The cage has composition $[(UO_2)_{50}(O_2)_{42}(WO_3OH)_6(H_2PO_4)_{20}(OH)_8(H_2O)_{18}]^{18-}$. The dimensions of the cluster are 21.7 by 24.5 Å, as measured from the outer edges of bounding O atoms.

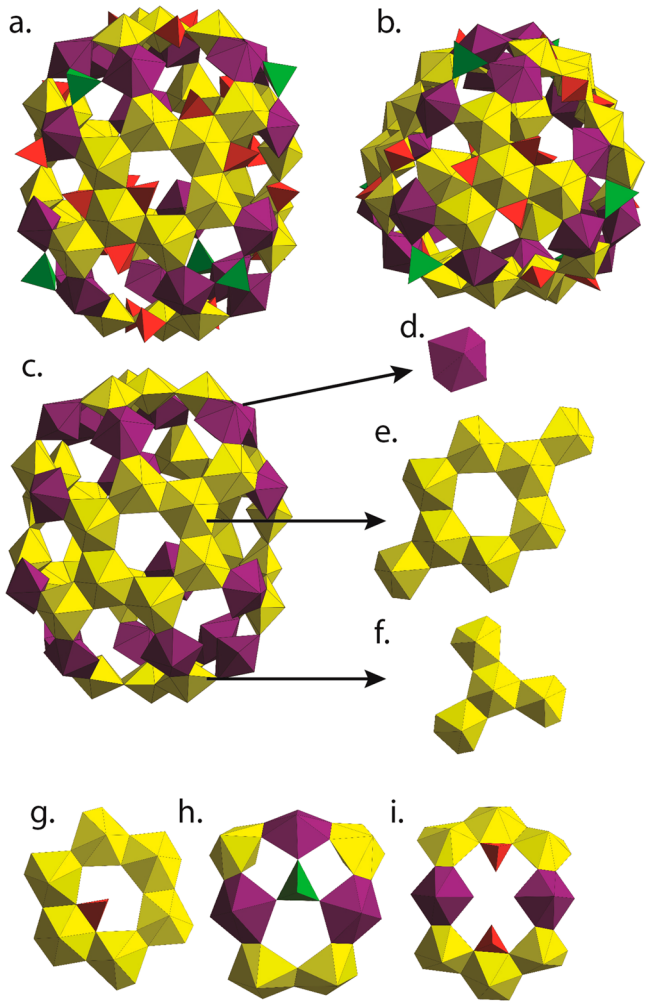

Figure 2. Polyhedral representations of cluster $U_{50}W_6P_{20}$ and its building units. Uranyl polyhedra that are connected to three and two other uranyl polyhedra are shown in yellow and purple, respectively. (a) Equatorial region. (b) Polar region. (c) Equatorial region with only the uranyl polyhedra shown. Phosphate tetrahedra and transition-metal polyhedra are shown in red and green, respectively.

The uranyl ions in $U_{50}W_6P_{20}$ are each present in hexagonal bipyramids, with five different coordination environments that correspond to those shown in Figure 1b,c,e,h,i. The connectivity of just the uranyl polyhedra is shown in Figure 2c. Thirty-two uranyl polyhedra share three of their edges with other uranyl polyhedra, and these are shown in yellow in Figure 2. These form two distinct structural units. One of these consists of eight 3-connected uranyl polyhedra, six of which form a six-membered ring by sharing edges (Figure 2e). Two 3-connected uranyl polyhedra are attached to the outside of the ring in a trans arrangement. There are three such units in the cluster, and they are distributed about the equatorial region in the representation given in Figure 2a. The other 3-connected uranyl polyhedra are located in the polar regions and form two tetramers in which the central uranyl polyhedron shares edges with each of the other three polyhedra (Figure 2f). These tetramers are a subunit of the eight-membered units described above. All of the 3-connected uranyl polyhedra either contain two bidentate peroxo ligands in a cis arrangement, or no peroxo ligands.

The structural units consisting of 3-connected uranyl polyhedra are linked into the $U_{50}W_6P_{20}$ cage cluster through 18 uranyl hexagonal bipyramids that contain two peroxo ligands in an unusual trans arrangement, shown in purple in Figure 2. Each of these is 2-connected to other uranyl polyhedra, with the result being both seven and eight-membered rings of edge-sharing uranyl bipyramids. Two $(H_2PO_4)^-$ ligands that are bidentate to uranyl ions project into the void space formed by each eight-membered ring (Figure 2i). A single $(H_2PO_4)^-$ ligand that is bidentate to a uranyl ion projects into the void space of each of the six-membered rings (Figure 2g). Each of the $(WO_3OH)^-$ tetrahedra occur in the middle of the seven-membered ring, where they share three of their vertices with adjacent uranyl polyhedra (Figure 2h).

The U−(O_2)−U dihedral angles are of particular importance where the bridge is peroxo, as a bent configuration is expected and provides the curvature that induces cage cluster formation.[37,38] The dihedral angles range from 129.9 to 146.2°.

3.5. The $U_{44}Mo_2P_{16}$ Cage Cluster. $U_{44}Mo_2P_{16}$ consists of 44 uranyl ions, 2 $(MoO_3OH)^{1-}$ tetrahedra, 14 $(H_2PO_4)^{1-}$ tetrahedra, and 2 $(HPO_4)^{2-}$ tetrahedra (Figure 3) and has composition $[(UO_2)_{44}(O_2)_{38}(H_2PO_4)_{14}(HPO_4)_2(MO_3OH)_2(OH)_{15}(H_2O)_{14}]^{23-}$, where protonation of the terminal O atoms bonded to Mo and P is assumed. Its dimensions are 19.2 by 25.1 Å, as measured from the outer edges of bounding O atoms. All of the uranyl ions are present in hexagonal bipyramids, but there are seven distinct coordination environments that correspond to those shown in Figure 1a,b,d,e,g,h,i.

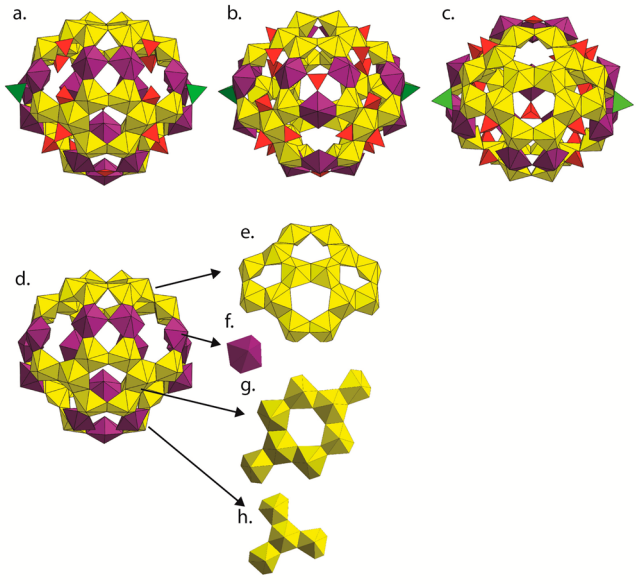

Figure 3. Polyhedral representations of cluster $U_{44}Mo_2P_{16}$ and its building units. Legend as in Figure 2. Panels (a) and (b) show equatorial views highlighting different coordination environments. (c) Polar view.

dx.doi.org/10.1021/ic5018449 | Inorg. Chem. 2014, 53, 12877−12884

The uranyl polyhedral portion of the cluster is shown in Figure 3d. Thirty of the hexagonal bipyramids share three equatorial edges with other bipyramids (shown in yellow), whereas 14 only share edges with two (shown in purple). Consider first the 3-connected polyhedra, which form three distinct structural units. Two of these are identical to the eight-membered unit and tetramer observed in $U_{50}W_6P_{20}$ (Figure 3g,h), although $U_{44}Mo_2P_{16}$ contains only one eight-membered unit and two tetramers. The third structural unit consists of 14 hexagonal bipyramids that are linked into two five-membered and two six-membered rings (Figure 3e). This configuration is a common feature in clusters built solely from uranyl polyhedra.[8] Note that the 3-connected uranyl polyhedra contain either one or two bidentate peroxo ligands. The 2-connected polyhedra each contains two peroxo ligands in a trans arrangement, where they link the structural units consisting of 3-connected polyhedra. In a departure from the connectivity themes of $U_{50}W_6P_{20}$, two of the uranyl hexagonal bipyramids that share only two edges with other bipyramids are linked through the sharing of a single vertex most clearly seen in Figure 3c,d. The result is a cage cluster that contains five-, six-, seven-, and eight-membered rings of edge-sharing uranyl polyhedra, as well as four-membered rings where the linkages are both through edge and vertex sharing.

The two $(MoO_3OH)^-$ tetrahedra and two $(HPO_4)^{2-}$ tetrahedra occur at the center of seven-membered rings, where they share vertices with three uranyl polyhedra, analogous to the $(WO_3OH)^-$ tetrahedra in $U_{50}W_6P_{20}$ (Figure 1h). Fourteen $(H_2PO_4)^{1-}$ tetrahedra are bidentate to uranyl ions and extend into the void space of the eight-membered rings of uranyl polyhedra, as in $U_{50}W_6P_{20}$ (Figure 1i).

Where the bridge between uranyl ions is bidentate peroxide, the U−(O_2)−U dihedral angles range from 126.4 to 147.5° in $U_{44}Mo_2P_{16}$.

3.6. The $U_{28}W_4P_{12}$ and $U_{28}Mo_4P_{12}$ Cage Cluster. $U_{28}W_4P_{12}$ consists of 28 uranyl ions, 4 $(WO_3OH)^-$ tetrahedra, and 12 $(H_2PO_4)^{2-}$ tetrahedra (Figure 4) and has composition

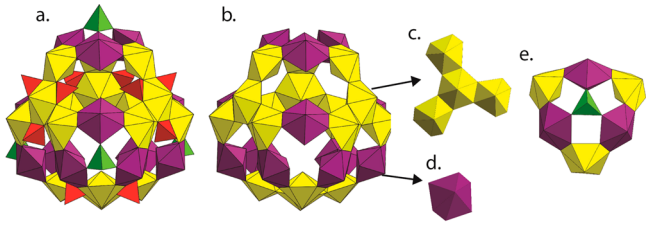

Figure 4. Polyhedral representations of cluster $U_{28}W_4P_{12}$ and $U_{28}Mo_4P_{12}$ and their building units. Legend as in Figure 2.

$[(UO_2)_{28}(O_2)_{24}(WO_3OH)_4(H_2PO_4)_{12}(H_2O)_{12}]^{20-}$, where all of the terminal O atoms bonded to P and W are assumed to be protonated. $U_{28}Mo_4P_{12}$ is derived from this cluster simply by replacing $(WO_3OH)^-$ by $(MoO_3OH)^-$. Its diameter is 19.6 Å, as measured from the outer edges of bounding O atoms. All of the uranyl ions are in hexagonal bipyramidal coordination environments. There are three distinct uranyl coordination environments corresponding to those shown in Figure 1c,e,i.

The uranyl polyhedral portion of $U_{28}W_4P_{12}$ is shown in Figure 4b. Uranyl hexagonal bipyramids either share three or two of their equatorial edges with other bipyramids. Considering first only the 3-connected bipyramids, shown in yellow, there is one distinct structural unit that is identical to the tetramers found in $U_{44}Mo_2P_{16}$ and $U_{50}W_6P_{20}$ (Figure 4c). Four such units occur in the cluster, where they are linked through 12 2-connected uranyl hexagonal bipyramids, all of which share trans peroxo edges with adjacent polyhedra (Figure 4d). As in $U_{44}Mo_2P_{16}$ and $U_{50}W_6P_{20}$, the connectivity of the uranyl polyhedra results in both six- and eight-membered rings of polyhedra.

The 12 $(H_2PO_4)^-$ tetrahedra in $U_{28}W_4P_{12}$ are structurally analogous to those in $U_{44}Mo_2P_{16}$ and $U_{50}W_6P_{20}$ in that they are bidentate to a uranyl ion and extend into the void space within the eight-membered rings of uranyl polyhedra (Figure 2i). The $(WO_3OH)^-$ tetrahedra are at the centers of the six-membered rings of uranyl polyhedra, where they share three of their vertices with uranyl polyhedra (Figure 4e). This configuration differs from that found in $U_{44}Mo_2P_{16}$ and $U_{50}W_6P_{20}$, in which the $(MoO_3OH)^-$ and $(WO_3OH)^-$ tetrahedra are at the centers of seven-membered rings (Figure 2h).

Where uranyl ions are bridged by bidentate peroxide, the U−(O_2)−U dihedral angles in $U_{28}W_4P_{12}$ range from 130.9 to 134.5°.

3.7. The $U_{18}W_2P_{12}$ Cage Cluster. $U_{18}W_2P_{12}$ consists of 18 uranyl ions, 2 $(WO_3(OH)_3)^{3-}$ octahedra, and 12 $(H_2PO_4)^-$ tetrahedra (Figure 5) and has composition $[(UO_2)_{18}(O_2)_{15}$-

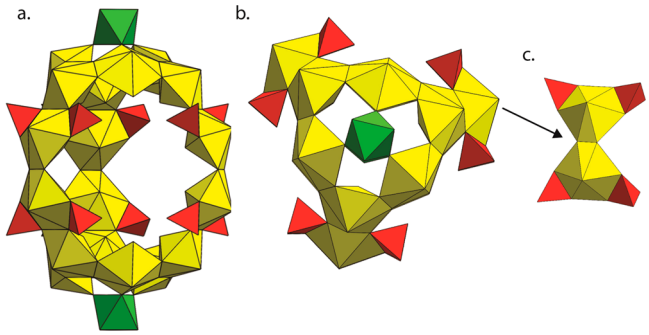

Figure 5. Polyhedral representations of cluster $U_{18}W_2P_{12}$ and its building units. Legend as in Figure 2.

$(W_2O_6(OH)_3)(H_2PO_4)_{12}(H_2O)_6]^{9-}$, where protonation of nonbridging O atoms bonded to W or P is assumed. Its diameter is 16.4 by 18.2 Å, as measured from the outer edges of bounding O atoms. The clusters are linked into a chain in the extended structure through the sharing of a face between $(WO_3(OH)_3)^{3-}$ octahedral, in contrast to all other reported uranyl peroxide cage clusters, which crystallize without direct linkages between them. The shared face corresponds to three symmetrically identical OH^- groups, with three identical W−O bond lengths of 2.18(1) Å. This general type of linkage of clusters into chains is also observed in transition-metal POM chemistry.[39,40] All of the uranyl ions are part of hexagonal bipyramids, with three different coordination environments that are shown in Figure 1c,e,f.

Only six of the uranyl hexagonal bipyramids in $U_{18}W_2P_{12}$ share edges with three other bipyramids, and the 3-connected polyhedra are isolated from each other. They are linked through 12 2-connected polyhedra; half have a single bidentate peroxo ligand, and the others have two bidentate peroxo ligands in a trans arrangement. Linkage of the uranyl polyhedra results in two six-membered rings at the polar regions of the cluster, and three 10-membered rings located about the equatorial region of the cluster.

The $(WO_3(OH)_3)^{3-}$ octahedra are located at the center of the six-membered rings of uranyl polyhedra, where they share

dx.doi.org/10.1021/ic5018449 | Inorg. Chem. 2014, 53, 12877−12884

three of their vertices with different uranyl polyhedra (Figure 5b). The $(H_2PO_4)^-$ tetrahedra are each bidentate to a uranyl ion, and four are directed into the void space within the 10-membered rings of uranyl polyhedra.

Where uranyl ions are bridged by bidentate peroxo ligands, the U−(O_2)−U dihedral angles range from 133.2 to 135.4°.

3.8. The $U_{48}W_6P_{48}$ Cage Cluster. $U_{48}W_6P_{48}$ consists of 48 uranyl ions, 6 $(WO_4OH)^{3-}$ square pyramids, 24 $(H_2PO_4)^-$ tetrahedra, and 24 $(HPO_4)^{2-}$ tetrahedra (Figure 6) and has composition $[(UO_2)_{48}(O_2)_{12}(WO_4OH)_6(H_2PO_4)_{24}(HPO_4)_{24}]^{18-}$, where it is assumed that all of the nonbridging O atoms bonded to W or P are protonated. Its diameter is 26.5 Å, as measured from the outer edges of bounding O atoms. Uranyl ions are present in both pentagonal and hexagonal bipyramids. Their coordination environments are shown in Figure 1f,j.

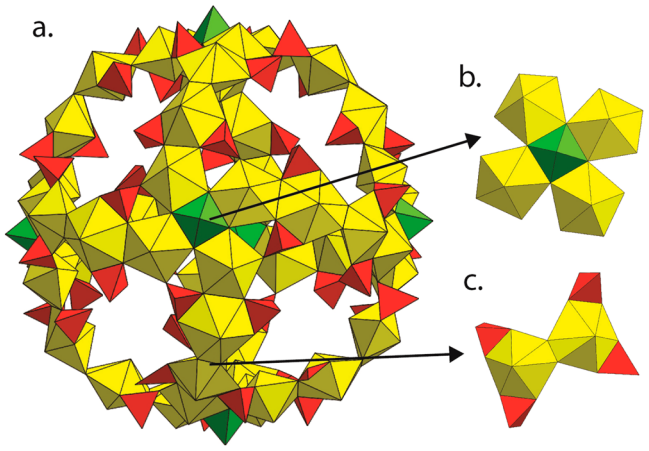

Figure 6. Polyhedral representations of cluster $U_{48}W_6P_{48}$ and its building units. Legend as in Figure 2.

In $U_{48}W_6P_{48}$ all of the uranyl hexagonal bipyramids share two equatorial edges with other bipyramids. Pentagonal bipyramids share one edge with a hexagonal bipyramid, and two vertices with two different pentagonal bipyramids. Although the cluster appears very complex in its representation, it consists of only two structural units that are defined in Figure 6. One of these is a four-membered ring of vertex-sharing pentagonal bipyramids, with a $(WO_4OH)^{3-}$ square pyramid located at the center of each ring, where it shares edges with each of the four uranyl bipyramids (Figure 6b). This unit is very similar to those found in dedecaniobate Keggin ions,[41] as well as in uranyl chromates.[42,43] The other structural unit consists of two uranyl hexagonal bipyramids that are bridged by a peroxo ligand that is bidentate to each uranyl ion. Each of these hexagonal bipyramids is also coordinated by two bidentate $(H_2PO_4)^{1-}$ tetrahedra (Figure 6c). These two structural units are linked by the sharing of polyhedral edges between uranyl pentagonal and hexagonal bipyramids, and single vertexes between $(HPO_4)^{2-}$ tetrahedra and uranyl pentagonal bipyramids. The result is a cage cluster with porous walls that contain the first examples of 12-membered rings of uranyl polyhedra.

4. DISCUSSION

The hybrid actinide−transition metal clusters reported here all self-assemble in aqueous solution under ambient conditions when uranyl nitrate, H_3PO_3, peroxide, and polyoxometalates containing either Mo or W are combined. Simple evaporation of the solutions eventually induces crystallization, which facilitated structure characterization. All of these clusters contain peroxo ligands that bridge between uranyl ions, which encourages formation of nanoscale cage clusters, rather than extended structures. The U−(O_2)−U dihedral angles of the peroxo bridges range from 126.4 to 147.5° in these clusters, consistent with our previously reported cage clusters as well as density function theory studies.[44−46]

The topologies of the clusters reported herein depart substantially from those based only on uranyl polyhedra.[8] Where cage clusters are built from uranyl polyhedra only, every polyhedron shares three of its equatorial edges, at least two of which correspond to peroxo ligands, with other uranyl polyhedra.[8] Several of these have fullerene topologies consisting of 12 topological pentagons as well as hexagons. Others include squares in their topologies, in combination with pentagons and

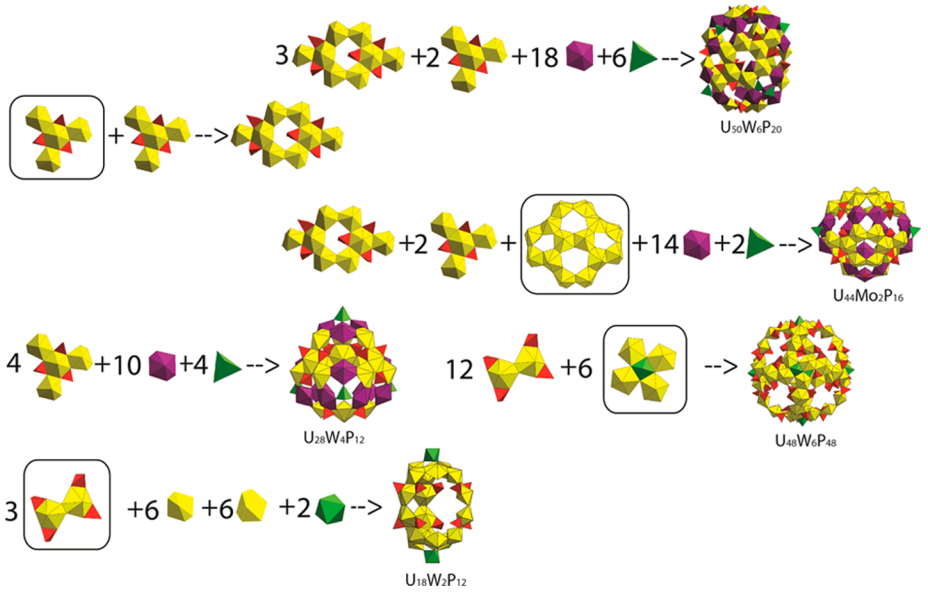

Figure 7. Polyhedral building units of uranyl peroxide phosphate transition-metal cage clusters under study. Legend as in Figure 2.

dx.doi.org/10.1021/ic5018449 | Inorg. Chem. 2014, 53, 12877−12884

hexagons. In clusters containing phosphate and transition metals, uranyl polyhedra are also connected into larger rings consisting of 7, 8, 10, or 12 members, as well as four- and six-membered rings that differ from those found previously in cage clusters, in which four uranyl ions are bridged by four bidentate peroxo ligands. The inclusion of uranyl hexagonal bipyramids with two peroxo ligands in a trans arrangement fosters formation of the larger rings and is an unusual feature that has only been found in two clusters previously.[47]

Self-assembly of topologically complex clusters such as those reported here likely involves the preformation of subunits in solution, and these may be influenced by the Li counterions. Possible assembly mechanisms, beginning with specific subunits built of uranyl polyhedra and phosphate tetrahedra, are shown for each cluster in Figure 7. Note that only two types of subunits are necessary, together with isolated polyhedra, to form clusters $U_{50}W_5P_{20}$, $U_{44}Mo_2P_{16}$, and $U_{28}W_4P_{12}$. In the case of $U_{18}W_2P_{12}$, one subunit is combined with isolated polyhedra. For $U_{48}W_6P_{48}$, two subunits only are required.

Each of the clusters reported here contains uranyl hexagonal bipyramids with two peroxo ligands in trans arrangements. These assume a fundamental structural role in the clusters, as they link uranyl polyhedra by sharing each of their bidentate peroxo ligands. Clusters built from uranyl polyhedra alone contain uranyl hexagonal bipyramids that have either two or three peroxo ligands. Where two are present, they are almost always in a cis configuration, and the bipyramid shares both of these, as well as a third edge defined by two hydroxyl groups, with other uranyl polyhedra. Such clusters self-assemble in alkaline aqueous solutions, with pH values in the range of 9–13. Topologically similar clusters where oxalate or pyrophosphate ligands bridge between uranyl polyhedra, rather than two hydroxyl groups, form over a broader range of pH, from 4 to 10. The major exception is found in two chiral uranyl peroxide cage clusters that are built dominantly from belts of uranyl polyhedra, in which some of the uranyl ions are bonded to two bidentate peroxo ligands in a trans arrangement.[47] These clusters formed in a solution with a pH of 6.0.

Studtite, $(UO_2)(O_2)(H_2O)_4$, forms when peroxide is added to acidic through circum-neutral aqueous solutions containing uranyl ions. It contains chains of uranyl hexagonal bipyramids that share peroxo ligands that are in trans arrangements about uranyl ions along the chain length.[48] H_2O groups occupy the other equatorial vertices also in a trans arrangement. As such, the uranyl ion coordination environment in studtite is very similar to that found for the trans peroxo uranyl hexagonal bipyramids in each of the clusters reported here. The only difference is that one equatorial H_2O group of the studtite configuration corresponds to an O atom of an oxyanion in the clusters. As such, it appears that the coordination of uranyl by two peroxide ligands in a trans arrangement is favored in aqueous solutions with acidic to circumneutral pH, with the cis arrangement of peroxide ligands dominant under alkaline conditions. Factors that influence the linkage of uranyl ions through peroxide under acidic conditions have not been rigorously evaluated. However, in the absence of alkali or alkaline earth counterions, studtite forms, but where counterions are present they may template formation of rings of uranyl ions bridged by peroxide, and therefore cage clusters.

Introduction of phosphate and tungstate or molybdate into cage clusters built from uranyl polyhedra has produced major topological departures from those clusters that are built only from uranyl polyhedra. Synthesis experiments conducted with similar systems under more alkaline conditions generally produced clusters built from uranyl polyhedra only. Reduction of the solution pH appears to favor uranyl hexagonal bipyramids with peroxo ligands in a trans arrangement, as discussed above. Such bipyramids have a profound impact on the topologies of the resulting clusters, arguably much more so than either the phosphate, tungstate, or molybdate polyhedra. The connectivities of the six cage clusters reported here have uranyl polyhedra that are linked directly to two or three other uranyl polyhedra, giving cages formed by the uranyl polyhedra alone (Figures 2–6) . The phosphate, tungstate, and molybdate oxyanions assume an essential role in stabilizing the clusters, both by bridging between different uranyl polyhedral units, and by coordinating the uranyl ions in specific ways to meet their bonding requirements.

The molybdate and tungstate do not appear to direct the formation of the clusters examined here, but rather they stabilize the observed configurations. Specifically, novel rings of seven uranyl polyhedra occur in $U_{50}W_6P_{20}$ and $U_{44}Mo_2P_{16}$ that contain three uranyl ions that are coordinated by two peroxide ligands in a trans configuration, and four containing two peroxide in cis configurations (Figures 2h and 3b). This relatively large ring is presumably stabilized by the $(WO_3OH)^-$ tetrahedron that lies within, where it shares vertices with each of three uranyl polyhedra that contain peroxide ligands in a trans arrangement. In $U_{28}W_4P_{12}$, $U_{28}Mo_4P_{12}$, and $U_{18}W_2P_{12}$ there are novel six-membered rings of uranyl polyhedra (Figures 4e and 6b). In previously reported uranyl peroxide cage clusters, six-membered rings invariably involved uranyl ions coordinated by two peroxide in a cis arrangement, or three peroxide. As such, the shared edges between uranyl polyhedra that defined the rings are also in a cis configuration, which gives a compact ring. In $U_{28}W_4P_{12}$, $U_{28}Mo_4P_{12}$, and $U_{18}W_2P_{12}$ six-membered rings of uranyl polyhedra contain uranyl ions with two peroxide ligands in a trans arrangement that are shared with adjacent uranyl ions, resulting in a more open ring. In $U_{28}W_4P_{12}$ and $U_{28}Mo_4P_{12}$ $(MoO_3OH)^-$ or $(WO_3OH)^-$ tetrahedra occur within these rings and presumably stabilize them, as each tetrahedron is linked to three different uranyl polyhedra of the ring. In the case of $U_{18}W_2P_{12}$, a $(WO_3(OH)_3)^{3-}$ octahedron is at the center of the six-membered ring, where it shares three O atoms with three different uranyl polyhedra.

In summary, uranyl peroxide cage clusters form under mildly acidic and circumneutral aqueous conditions in the presence of phosphate, molybdate, or tungstate and adopt new cage topologies that incorporate transition-metal polyhedra within the cage walls. These clusters contain larger rings of uranyl polyhedra than those that contain only uranyl polyhedra, and provide rare examples of clusters that contain uranyl ions coordinated by two bidentate peroxo ligands in a trans arrangement.

■ ASSOCIATED CONTENT

Supporting Information

Infrared spectra, crystallographic details, and CIF files. This material is available free of charge via the Internet at http://pubs.acs.org.

■ AUTHOR INFORMATION

Corresponding Author

*E-mail: pburns@nd.edu.

Notes

The authors declare no competing financial interest.

■ ACKNOWLEDGMENTS

This material is based upon work supported as part of the Materials Science of Actinides Center, an Energy Frontier Research Center funded by the U.S. Department of Energy, Office of Science, Office of Basic Energy Sciences under Award Number DE-SC0001089.

■ REFERENCES

(1) Hill, C. L.; Prossermccartha, C. M. *Coord. Chem. Rev.* **1995**, *143*, 407.
(2) Long, D. L.; Burkholder, E.; Cronin, L. *Chem. Soc. Rev.* **2007**, *36*, 105.
(3) Long, D. L.; Tsunashima, R.; Cronin, L. *Angew. Chem., Int. Ed.* **2010**, *49*, 1736.
(4) Neumann, R. *Prog. Inorg. Chem.* **1998**, *47*, 317.
(5) Pope, M. T.; Muller, A. *Angew. Chem., Int. Ed. Engl.* **1991**, *30*, 34.
(6) Qi, W.; Wu, L. X. *Polym. Int.* **2009**, *58*, 1217.
(7) Nyman, M.; Burns, P. C. *Chem. Soc. Rev.* **2012**, *41*, 7354.
(8) Qiu, J.; Burns, P. C. *Chem. Rev.* **2013**, *113*, 1097.
(9) Burns, P. C. *Mineral. Mag.* **2011**, *75*, 1.
(10) Burns, P. C.; Kubatko, K. A.; Sigmon, G.; Fryer, B. J.; Gagnon, J. E.; Antonio, M. R.; Soderholm, L. *Angew. Chem., Int. Ed.* **2005**, *44*, 2135.
(11) Burns, P. C.; Ewing, R. C.; Navrotsky, A. *Science* **2012**, *335*, 1184.
(12) Kubatko, K. A. H.; Helean, K. B.; Navrotsky, A.; Burns, P. C. *Science* **2003**, *302*, 1191.
(13) Qiu, J.; Ling, J.; Jouffret, L.; Thomas, R.; Szymanowski, J. E. S.; Burns, P. C. *Chem. Sci.* **2014**, *5*, 303.
(14) Wylie, E. M.; Peruski, K. M.; Weidman, J. L.; Phillip, W. A.; Burns, P. C. *ACS Appl. Mater. Interfaces* **2013**, *6*, 473.
(15) Yanagie, H.; Ogata, A.; Mitsui, S.; Hisa, T.; Yamase, T.; Eriguchi, M. *Biomed. Pharmacother.* **2006**, *60*, 349.
(16) Alizadeh, M. H.; Mohadeszadeh, M. *J. Cluster Sci.* **2008**, *19*, 435.
(17) Antonio, M. R.; Chiang, M. H. *Inorg. Chem.* **2008**, *47*, 8278.
(18) Chiang, M. H.; Soderholm, L.; Antonio, M. R. *Eur. J. Inorg. Chem.* **2003**, 2929.
(19) Chiang, M. H.; Williams, C. W.; Soderholm, L.; Antonio, M. R. *Eur. J. Inorg. Chem.* **2003**, 2663.
(20) Gaunt, A. J.; May, I.; Collison, D.; Holman, K. T.; Pope, M. T. *J. Mol. Struct.* **2003**, *656*, 101.
(21) Khoshnavazi, R.; Eshtiagh-Hossieni, H.; Alizadeh, M. H.; Pope, M. T. *Polyhedron* **2006**, *25*, 1921.
(22) Mohadeszadeh, M. *J. Cluster Sci.* **2011**, *22*, 183.
(23) Gaunt, A. J.; May, I.; Copping, R.; Bhatt, A. I.; Collison, D.; Fox, O. D.; Holman, K. T.; Pope, M. T. *Dalton Trans.* **2003**, 3009.
(24) Mal, S. S.; Dickman, M. H.; Kortz, U. *Chem.—Eur. J.* **2008**, *14*, 9851.
(25) Mishra, A.; Abboud, K. A.; Christou, G. *Inorg. Chem.* **2006**, *45*, 2364.
(26) Mishra, A.; Tasiopoulos, A. J.; Wernsdorfer, W.; Abboud, K. A.; Christou, G. *Inorg. Chem.* **2007**, *46*, 3105.
(27) Miro, P.; Ling, J.; Qiu, J.; Burns, P. C.; Gagliardi, L.; Cramer, C. J. *Inorg. Chem.* **2012**, *51*, 8784.
(28) Nyman, M.; Rodriguez, M. A.; Alam, T. M. *Eur. J. Inorg. Chem.* **2011**, 2197.
(29) Bruker, 2001.
(30) *APEX2*; Bruker AXS Inc.: Madison, Wisconsin, USA, 2007.
(31) Sheldrick, G. M. Bruker AXS, Inc.: Madison, WI, USA, 1996.
(32) Alam, T. M.; Liao, Z. L.; Zakharov, L. N.; Nyman, M. *Chem.—Eur. J.* **2014**, *20*, 8302.
(33) Brown, I. D.; Altermatt, D. *Acta Crystallogr., Sect. B* **1985**, *41*, 244.
(34) Burns, P. C.; Ewing, R. C.; Hawthorne, F. C. *Can. Mineral.* **1997**, *35*, 1551.
(35) Balboni, E.; Burns, P. C. *J. Solid State Chem.* **2014**, *213*, 1.
(36) Seliverstov, A. N.; Suleimanov, E. V.; Chuprunov, E. V.; Somov, N. V.; Zhuchkova, E. M.; Lelet, M. I.; Rozov, K. B.; Depmeier, W.; Krivovichev, S. V.; Alekseev, E. V. *Dalton Trans.* **2012**, *41*, 8512.
(37) Sigmon, G. E.; Ling, J.; Unruh, D. K.; Moore-Shay, L.; Ward, M.; Weaver, B.; Burns, P. C. *J. Am. Chem. Soc.* **2009**, *131*, 16648.
(38) Vlaisavljevich, B.; Gagliardi, L.; Burns, P. C. *J. Am. Chem. Soc.* **2010**, *132*, 14503.
(39) Bonhomme, F.; Larentzos, J. P.; Alam, T. M.; Maginn, E. J.; Nyman, M. *Inorg. Chem.* **2005**, *44*, 1774.
(40) Nyman, M.; Bonhomme, F.; Alam, T. M.; Rodriguez, M. A.; Cherry, B. R.; Krumhansl, J. L.; Nenoff, T. M.; Sattler, A. M. *Science* **2002**, *297*, 996.
(41) Hou, Y.; Zakharov, L. N.; Nyman, M. *J. Am. Chem. Soc.* **2013**, *135*, 16651.
(42) Unruh, D. K.; Quicksall, A.; Pressprich, L.; Stoffer, M.; Qiu, J.; Nuzhdin, K.; Wu, W. Q.; Vyushkova, M.; Burns, P. C. *J. Solid State Chem.* **2012**, *191*, 162.
(43) Sykora, R. E.; Albrecht-Schmitt, T. E. *J. Solid State Chem.* **2004**, *177*, 3729.
(44) Gil, A.; Karhanek, D.; Miro, P.; Antonio, M. R.; Nyman, M.; Bo, C. *Chem.—Eur. J.* **2012**, *18*, 8340.
(45) Miro, P.; Bo, C. *Inorg. Chem.* **2012**, *51*, 3840.
(46) Miro, P.; Pierrefixe, S.; Gicquel, M.; Gil, A.; Bo, C. *J. Am. Chem. Soc.* **2010**, *132*, 17787.
(47) Qiu, J.; Nguyen, K.; Jouffret, L.; Szymanowski, J. E. S.; Burns, P. C. *Inorg. Chem.* **2013**, *52*, 337.
(48) Burns, P. C.; Hughes, K. A. *Am. Mineral.* **2003**, *88*, 1165.